

Invasive growth of Co on $(\sqrt{2} \times \sqrt{2})R45^\circ$ reconstructed O/Cu(001)

Xiangdong Liu,^{a)} Takushi Iimori, Kan Nakatsuji, and Fumio Komori
*Institute for Solid State Physics, University of Tokyo, Kashiwanoha 5-1-5, Kashiwashi,
 Chiba 277-8581, Japan*

(Received 30 November 2005; accepted 6 February 2006; published online 27 March 2006)

Submonolayer growth of Co on the reconstructed Cu(001) $(\sqrt{2} \times \sqrt{2})R45^\circ$ -O surface has been investigated by scanning tunneling microscopy. Cu atoms are displaced from the Cu(001) $(\sqrt{2} \times \sqrt{2})R45^\circ$ -O structure by incoming Co atoms and subsequently aggregate into elongated islands. The deposited Co atoms are randomly distributed in the oxygen adsorbed surface as individual atoms and clusters at low coverages [≤ 0.4 monolayers (ML)]. For larger coverages (≥ 0.5 ML), compact fcc Co patches are formed. The adsorbed oxygen acts as a surfactant. Interfacial intermixing is reduced when Co is deposited on the Cu(001) $(\sqrt{2} \times \sqrt{2})R45^\circ$ -O surface. © 2006 American Institute of Physics. [DOI: 10.1063/1.2189190]

It is well known that adsorbed gases influence the epitaxial growth of metals on metals.¹ Recently, preadsorbed and well-ordered oxygen atoms have been used as a surfactant in the growth of ultrathin 3d ferromagnetic films on a Cu substrate.²⁻⁴ In this way, smooth layer-by-layer growth has been achieved for Co and Ni on Cu(110) (2×1) -O.^{2,5} On reconstructed Cu(001) $(\sqrt{2} \times \sqrt{2})R45^\circ$ -O, Ni growth was almost a perfect two-dimensional (2D) growth compared with that on clean Cu(001).⁶ On the other hand, the effects of the oxygen-induced reconstruction on the initial growth and thus the interface structure have not been extensively studied so far. However, a precise control of the interface structure is required for applications such as electronic and spintronic devices. An typical example is that the giant magnetoresistance effect in the Co/Cu multilayers significantly depends on their interfacial properties.^{7,8}

In this letter, we have investigated the initial growth of Co on the Cu(001) $(\sqrt{2} \times \sqrt{2})R45^\circ$ -O surface using scanning tunneling microscopy (STM). The growth is characterized by two processes. One is the displacement of Cu atoms by the arriving Co atoms. The released Cu atoms aggregate into elongated islands. The other is the formation of the Co(001) $c(2 \times 2)$ -O structure. With ordered oxygen atoms on the surface as the surfactant, the intermixing between Cu and Co is reduced. This contrasts with the formation of an atomically mixed interface when Co is deposited on clean Cu(001).⁹

The experiments were carried out in an ultrahigh vacuum apparatus equipped with a Rastroscope-3000 STM and a four-grid low-energy electron diffraction (LEED) optics. The Cu(001) $(\sqrt{2} \times \sqrt{2})R45^\circ$ -O surface was prepared by exposing the clean Cu(001) surface to 3000–6000 l of oxygen molecules at 523 K. Its structure is schematically shown in Fig. 1. Cobalt was deposited by an electron-bombardment evaporator from a 99.99% pure wire. The depositions were done at room temperature (RT) except where noted. The deposition rate was 0.3 monolayers (ML)/min. All the STM images were recorded in the constant current mode at RT using a Pt/Ir tip.

The result for a 0.05-ML Co deposited sample is shown in Fig. 2(a). On this sample, we notice two features. One is

the elongated islands which are oriented along the [100] or [010] direction. The other is the atoms or clusters scattered on the surface. We first focus on the islands. In Fig. 2(b), the surface structure of an island is atomically resolved. It turns out to be the $(\sqrt{2} \times \sqrt{2})R45^\circ$ structure. Since this oxygen-adsorbed structure is formed only on Cu(001) but not on Co, we can conclude that the islands are resulted from the aggregation of Cu atoms. From this it can be deduced that the scattered atoms are Co. We will further confirm this point later.

Now we turn our attention to the scattered Co atoms. Shown in Figs. 2(c) and 2(d) are two STM images extracted from a 2-h-long STM movie. The time interval between them is 115 min. By comparing the relative positions of the Co atoms, one can find that they never move. In contrast to the immobility of the Co atoms, the domain boundary of the reconstructed surface (refer to Fig. 1) migrates rapidly (but never passes across the positions occupied by Co atoms). Since the migration of the domain boundary results from Cu hopping, it can be inferred that Cu atoms are mobile. This is in agreement with our conclusion that the elongated islands are constructed by Cu atoms, since only mobile atoms can form islands.

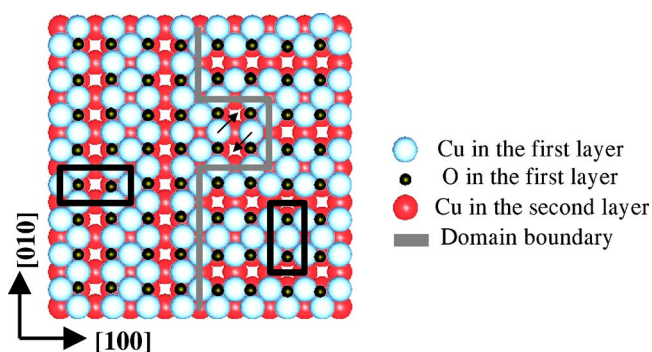


FIG. 1. (Color online) (a) The Cu(001) $(\sqrt{2} \times \sqrt{2})R45^\circ$ -O surface structure is schematically shown. The unit cells are specified using black rectangles. This surface contains 0.75 ML Cu and 0.5 ML O. Two reconstruction domains can be observed with the orientation of their unit cell perpendicular to each other. The domain boundary is denoted by grey thick lines. The arrows show the Cu hopping which will lead to the migration of the domain boundary.

^{a)}Electronic mail: xiang@issp.u-tokyo.ac.jp

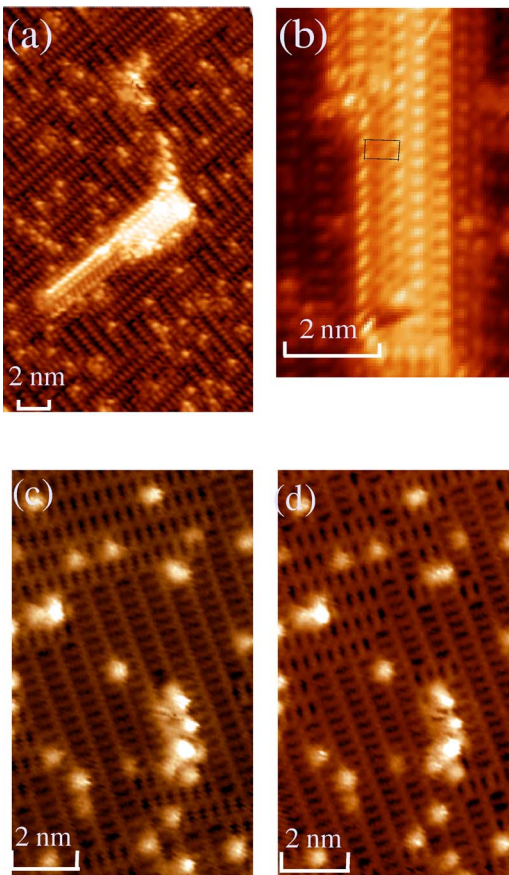


FIG. 2. (Color online) (a) After 0.05 ML of Co was deposited on the $\text{Cu}(001)(\sqrt{2}\times 2\sqrt{2})R45^\circ\text{-O}$ surface, elongated islands as well as scattered individual atoms and clusters are observed. (b) Atomically resolved STM image of the island surface. The $(\sqrt{2}\times 2\sqrt{2})R45^\circ$ unit cell is marked using a black rectangle. (c) and (d) Two STM images extracted from a STM movie with a time interval of 115 min. The constant relative positions show the scattered Co atoms are immobile.

In Figs. 3(a)–3(c), we present the typical STM images which summarize the submonolayer growth of Co on $\text{Cu}(001)(\sqrt{2}\times 2\sqrt{2})R45^\circ\text{-O}$ at RT. With increasing Co amount, the coverage of Cu islands simply increases. On the other hand, the Co atoms show a complicated behavior. At 0.2 ML Co, they still distribute randomly as individual atoms and clusters [Fig. 3(a)], similar to those on the 0.05-ML sample. The density of Co clusters increases obviously when the Co amount is raised to 0.4 ML [Fig. 3(b)]. When we further increase the Co amount, the Co clusters start to aggregate into ordered and compact patches. At 0.6-ML Co, well-developed Co patches are formed adjacent to the Cu islands [smooth areas on the terrace in Fig. 3(c)]. The patches show a $c(2\times 2)$ structure as shown in the magnified image, Fig. 3(d). Since it is well established that a half monolayer of oxygen on fcc Co adopts a $c(2\times 2)$ structure,¹⁰ the observed $c(2\times 2)$ structure assures that the patches are really constructed by Co atoms with oxygen floated on them.

The observation of elongated Cu islands after Co deposition gives rise to the question: where do these Cu atoms come from? The most reasonable answer is that Cu atoms are released upon the accommodation of the deposited Co atoms. To confirm this argument and to obtain more information about Cu ejection, we have quantitatively measured the coverage of the Cu islands as a function of the amount of the deposited Co. Interestingly, a proportionality close to 0.75

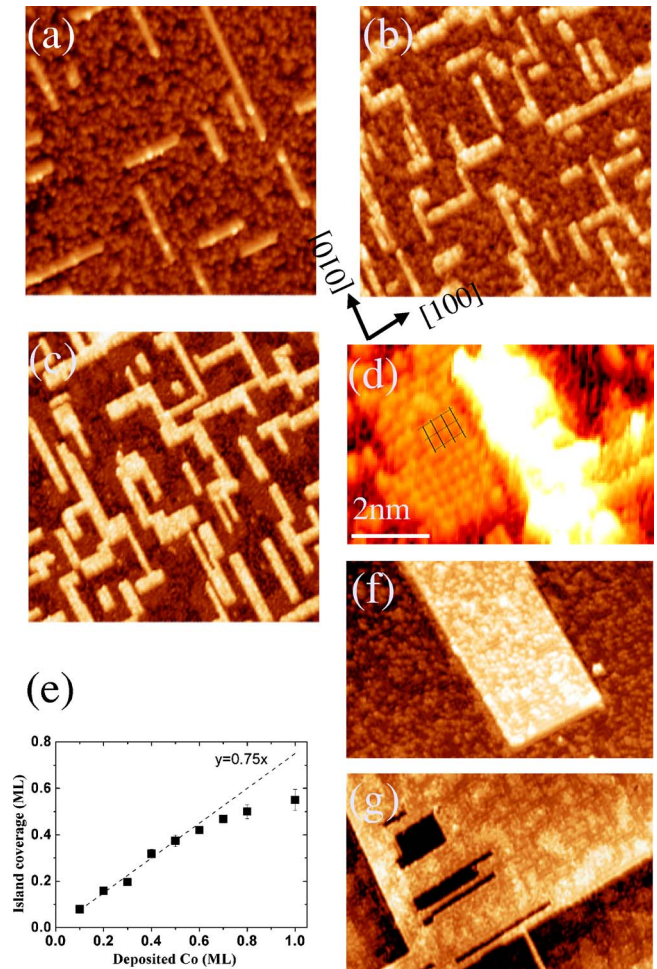


FIG. 3. (Color online) (a)–(c) STM images for (a) 0.2-, (b) 0.4-, and (c) 0.6-ML Co deposited at RT. The image size is $25\times 25\text{ nm}^2$. (d) A STM image showing the $c(2\times 2)$ structured Co patches for the 0.6-ML sample. (e) The statistical island coverage is plotted vs the amount of deposited Co. The broken line with a slope of 0.75 is a guide for the eye. (f) and (g) STM images of 0.2- and 0.45-ML Co deposited at 450 and 370 K, respectively. The images have a size of $25\times 16\text{ nm}^2$.

was obtained up to 0.6-ML deposited Co as shown in Fig. 3(e). It is noted that the Cu coverage on the clean $(\sqrt{2}\times 2\sqrt{2})R45^\circ$ surface is 0.75 ML. Thus, the observed proportionality means that the Co clusters and $c(2\times 2)$ patches are grown on driving away all the $(\sqrt{2}\times 2\sqrt{2})R45^\circ$ structured Cu atoms in there. The released Cu atoms finally aggregate into islands. We notice that the proportionality downwards deviates from 0.75 when more than 0.6 ML of Co is deposited. The deviation is caused by the reduced capture probability of the grown Cu islands after the $c(2\times 2)$ patches start to form on the terrace.

It has also been found during the formation of Cu islands that the Co atoms, which have already been there, float onto the island surface. The floating up of Co atoms are seen as the protrusions on the Cu islands shown in Figs. 3(a)–3(c). The density of the Co atoms on the island is the same as that on the terrace. This can be more clearly demonstrated at raised deposition temperatures, which allow wide Cu islands to form due to the increased diffusion length of the Cu atoms. We observed the identical density of Co atoms and the same morphology both on the island and on the terrace as shown in Fig. 3(f). At the same time, rectangular peninsulas and grooves appear on the upper terrace near the step at

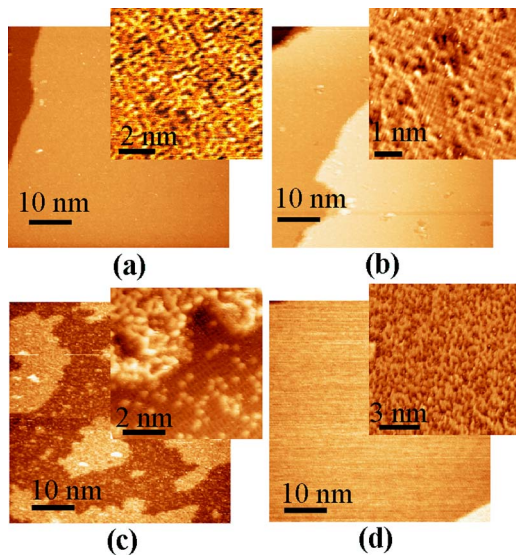


FIG. 4. (Color online) STM images resulted after (a) 0.45-ML Co deposited at 460 K on clean Cu(001), (b) 0.45-ML Co deposited at 460 K on clean Cu(001) and annealed at 520 K for 120 min, (c) 0.45-ML Co deposited at 460 K and subsequently exposed to 4000 l oxygen at RT and finally annealed at 520 K for 120 min, (d) the sample used for (c) was further annealed at 570 K for 60 min.

elevated deposition temperature [see Fig. 3(g)]. These two features tell us that the terrace (including the peninsulas), which is adjacent to a descending step, was newly grown during the Co deposition. Again, the newly formed area has the same coverage of the $c(2 \times 2)$ Co patches as in other places. All these results clearly indicate the floating up of Co atoms. Additionally, the same image contrast for the newly formed area as that for the original terrace in these figures confirms our conclusion that the islands are produced by Cu aggregation.

We notice that, after forming the $c(2 \times 2)$ Co patch, Cu and Co atoms are well separated without intermixing at the interface. This is sharply contrasted with the case of Co deposition on clean Cu(001), where a considerable amount of Co is incorporated into the Cu(001) substrate and thus results in an intermixed interface.⁹ We can further show that the absence of intermixing is thermodynamically ensured for the oxygen adsorbed submonolayer Co/Cu(001) films. As shown in Fig. 4(a), a deposition at 460 K of 0.45 ML Co on clean Cu(001) results in an island-free and an atomically intermixed surface. The intermixed surface remains after an-

nealing the sample at 520 K for 120 min [Fig. 4(b)]. However, when the surface is exposed to 4000 l oxygen at RT before the annealing, it turns out to be separated into $(\sqrt{2} \times 2\sqrt{2})R45^\circ$ -Cu areas and Co-rich areas after the annealing [Fig. 4(c)]. Further annealing the sample at 570 K for 60 min restores the intermixed surface because of the desorption of oxygen [Fig. 4(d)]. This experiment clearly demonstrated that the intermixed structure is thermodynamically unstable at the presence of oxygen.

In summary, we have investigated the submonolayer growth of Co on Cu(001) $(\sqrt{2} \times 2\sqrt{2})R45^\circ$ -O. The growth is characteristic of the displacement of Cu atoms by the incoming Co atoms. The displaced Cu atoms aggregate into elongated rectangular islands. With oxygen floated onto it through an exchange process, the Co overlayer is grown subsequently on driving away the $(\sqrt{2} \times 2\sqrt{2})R45^\circ$ structured Cu atoms in there. By forming Cu islands and Co patches separately, interfacial intermixing is reduced for the growth of Co on Cu(001) at the presence of oxygen.

The authors thank D. Sekiba for fruitful discussions. One of the authors (X.L.) acknowledges the support from Japan Society for the Promotion of Science.

¹W. F. Egelhoff, Jr. and D. A. Steigewald, *J. Vac. Sci. Technol. A* **7**, 2167 (1989).

²Ch. Tölkes, R. Struck, R. David, P. Zeppenfeld, and G. Comsa, *Phys. Rev. Lett.* **80**, 2877 (1998); R. Nünthel, J. Lindner, P. Pouloupoulos, and K. Baberschke, *Surf. Sci.* **566–568**, 100 (2004).

³B. B. Maranville and F. Hellman, *Appl. Phys. Lett.* **81**, 4011 (2002).

⁴J. Hong, R. Q. Wu, J. Lindner, E. Kosubek, and K. Baberschke, *Phys. Rev. Lett.* **92**, 147202 (2004); R. Nünthel, J. Lindner, P. Pouloupoulos, and K. Baberschke, *Surf. Sci.* **531**, 53 (2003).

⁵C. Sorg, N. Ponpandian, A. Scherz, H. Wende, R. Nünthel, T. Gleitsmann, and K. Baberschke, *Surf. Sci.* **565**, 197 (2004).

⁶J. Linder, P. Pouloupoulos, R. Nünthel, E. Kosubek, H. Wende, and K. Baberschke, *Surf. Sci.* **523**, L65 (2003).

⁷C. Blaas, L. Szunyogh, P. Weinberger, C. Sommers, P. M. Levy, and J. Shi, *Phys. Rev. B* **65**, 134427 (2002); H. D. Chopra, D. X. Yang, P. J. Chen, and W. F. Egelhoff, *Phys. Rev. B* **65**, 094433 (2002).

⁸K. Kagawa, H. Kano, A. Okabe, A. Suzuki, and K. Hayashi, *J. Appl. Phys.* **75**, 6540 (1994); W. F. Egelhoff, Jr., P. J. Chen, C. J. Powell, M. D. Stiles, R. D. McMichael, J. H. Judy, K. Takano, and A. E. Berkowitz, *J. Appl. Phys.* **82**, 6142 (1997); S. Miura, M. Tsunoda, and M. Takahashi, *ibid.* **89**, 6308 (2001); D. J. Larson, A. K. Petford-Long, A. Cerezo, S. P. Bozeman, A. Morrone, Y. Q. Ma, A. Georgalakis, and P. H. Clifton, *Phys. Rev. B* **67**, 144420 (2003).

⁹F. Nouvertin, U. May, M. Bammig, A. Rampe, U. Korte, G. Gntherodt, R. Pentcheva, and M. Scheffler, *Phys. Rev. B* **60**, 14382 (1999).

¹⁰K. G. Nath, Y. Haruyama, and T. Kinoshita, *Surf. Sci.* **486**, 185 (2001).